AAS 16-495

NONLINEAR ANALYTICAL EQUATIONS OF RELATIVE MOTION ON J_2-PERTURBED ECCENTRIC ORBITS

Bradley Kuiack* **and Steve Ulrich†**

Future spacecraft formation flying missions will require accurate autonomous guidance systems to calculate a reference, or desired, relative motion during reconfiguration maneuvers. However, the efficiency in terms of propellant used for such maneuvers depends on the fidelity of the dynamics model used for calculating the reference relative motion. Therefore, an efficient method for calculating relative motion should have an analytical solution, be applicable to an eccentric orbit, and should take into account the J_2 perturbation. This paper accomplishes this through an exact analytical solution of the relative motion between two spacecraft based on the orbital elements of each spacecraft. Specifically, by propagating the J_2-perturbed osculating orbital elements forward in time and solving the exact solution at each time step, an accurate representation of the true spacecraft relative motion is obtained. When compared to a numerical simulator, the proposed analytical solution is shown to accurately model the relative motion, with bounded errors on the order of meters over a wide range of eccentricity values.

INTRODUCTION

Formation flying of multiple spacecraft is a key enabling technology for many future scientific missions such as enhanced stellar optical interferometers and virtual platforms for Earth or Sun observations. However, formation flying involves several considerations beyond those of a single spacecraft mission. This is particularly true for the guidance system, which is responsible for calculating a reference, or desired, relative motion to be actively tracked during reconfiguration maneuvers by the on-board control system of a follower spacecraft. Such guidance systems require accurate but simple dynamics models of the spacecraft relative motion. Specifically, the dynamics models have to be accurate enough to prevent unnecessary fuel expenditure, as ignoring perturbations in the design of the reference relative trajectories will most likely result in additional propellant consumption to force the follower spacecraft to track artificial reference trajectories. Indeed, to limit the propellant consumption, the follower spacecraft must avoid compensating for orbital perturbations, as well as other nonlinear effects inherent to large separation distances and/or eccentricity values. In other words, the effectiveness of a reference relative motion depends on the accuracy of the dynamics model used for its design. In addition, the guidance system must remain computationally simple for on-board implementation purposes. As such, analytical solutions are preferable as they do not rely on numerical integrations.

*Undergraduate Student, Department of Mechanical and Aerospace Engineering, Carleton University, 1125 Colonel By Drive, Ottawa, ON, K1S 5B6, Canada.

†Assistant Professor, Department of Mechanical and Aerospace Engineering, Carleton University, 1125 Colonel By Drive, Ottawa, ON, K1S 5B6, Canada.

While some analytical solutions to the exact nonlinear differential equations of relative motion in the local-vertical-local-horizontal reference frame do exist, they nevertheless impose certain restrictions in their derivations. For example, the Hill-Clohessy-Wiltshire (HCW) model,[1] does have a time-explicit closed-form analytical solution to the relative motion problem, but only for circular Keplerian orbits. Sabol and McLaughlin[2] reparametrized this model and demonstrated that the in-plane and out-of-plane non-drifting relative motion about a circular Keplerian orbit always follows an ellipse centered on the reference orbit.

To overcome the inherent limitations of the HCW model, some formulations also take into account orbit perturbations, notably the perturbation caused by the oblateness of the Earth, referred to as the J_2 perturbation. The J_2 perturbation is particularly important in formation flying since its secular effect on an orbit, i.e., the rotation of the line of apsides and precession of the line of nodes, causes secular drift between two J_2-perturbed spacecraft. The introduction of J_2 in a linearized set of equations, similar to the HCW equations, has been proposed by Schweighart and Sedwick.[3] Specifically, the authors developed a set of linear, constant-coefficient, second-order differential equations of motion by considering the orbit-averaged impact of J_2 on a circular reference orbit. An analytical solution to these differential equations is also presented.

However, assuming a circular reference orbit yields considerable errors when the eccentricity of the reference orbit increases. In fact, it has been shown that the errors introduced in the HCW equations by considering an elliptical reference orbit dominate the errors due to ignoring J_2.[4] For this reason, several formulations have been proposed to model the relative motion about unperturbed elliptical orbits.[5–7] In particular, the linear-time-invariant (LTI) HCW equations have been extended to arbitrary eccentricity by Inalhan et al.[4] by formulating the dynamics as a linear-parameter-varying (LPV) system. Such a dynamics model is especially well suited for controller design purposes, by making use of LPV control techniques, such as model predictive control.[8] Making use of the fact that the orbit angular rate and the radius are functions of the true anomaly, these equations can also be expressed using true anomaly derivatives instead of time derivatives.[9] The resulting differential equations are also time-varying, but are not parameter-varying since the true anomaly has been used to formulate the derivatives. Solutions to these linear-time-varying (LTV) equations are available in the literature in various forms using different reference frames and variables. The first derivation with singularities in the closed-form solution was provided by Lawden.[10] Then, Carter[11] provided a set of solutions without singularities. These homogenous solutions are extremely useful for well-behaved numerical and analytical analysis on the shape, structure, and optimization of passive apertures in eccentric reference orbits. Interestingly, the same solutions can be obtained via incremental changes in orbital elements, as demonstrated by Marec.[12] Lane and Axelrad[13] developed a time-explicit closed-form solution and studied the relative motion for bounded elliptical orbits. Melton[14] also proposed an alternative solution for small eccentricity reference orbits. More recently, an elegant closed-form analytical solution that is valid for Keplerian eccentric orbits was developed by Gurfil and Kholshevnikov.[15,16] This simple analytical solution explicitly parameterizes the relative motion using classical orbital elements as constants of the unperturbed Keplerian orbit, instead of Cartesian initial conditions. This concept, originally suggested by Hill,[17] has been widely used in the analysis of relative spacecraft dynamics.[18,19] A key advantage of this approach is that it facilitates the inclusion of the orbital perturbation effects on the relative motion.

In this context, the original contribution of this paper is to propose an improvement to Gurfil and Kholshevnikov's equations of relative motion[15,16] by taking into account J_2 perturbation. This is achieved by using J_2-perturbed osculating orbital elements in their solutions instead of using

constant orbital elements. The osculating orbital elements are calculated by adding the mean orbital elements to the J_2-induced short-periodic variations.[20,21] In addition, the original solution by Gurfil and Kholshevnikov was not fully analytical as numerical integrations were employed to calculate the true anomaly of the leader spacecraft and the eccentric anomaly of the follower spacecraft.[15,16] This problem is herein alleviated by using an analytical approximation of the eccentric anomalies, which is then used to calculate the true anomalies of both spacecraft.

NONLINEAR ANALYTICAL EQUATIONS OF RELATIVE MOTION

This section details the methods used to derive a set of nonlinear analytical equations of relative motion which are applicable to J_2 perturbed eccentric orbits.

Reference Frames

For completeness, the reference frames that will be subsequently used in the derivations of the equations of motion are first introduced.

The first is the Earth-centered inertial (ECI) reference frame, denoted by $\mathcal{F}_I$ and defined by its orthonormal unit vectors $\left\{\vec{I}_x, \vec{I}_y, \vec{I}_z\right\}$. This reference frame has its origin at the center of the Earth, its $\vec{I}_z$ is along the Earth's polar axis of rotation, and its $\vec{I}_x$ and $\vec{I}_y$ unit vectors in the Earth's equatorial plane. Specifically, the unit vector $\vec{I}_x$ of ECI is along the vernal equinox line in the direction of the vernal equinox (sometimes called the first point of Aries), and $\vec{I}_y = \vec{I}_z \times \vec{I}_x$.

The perifocal frame, denoted by $\mathcal{F}_P$ and defined by its orthonormal unit vectors $\left\{\vec{P}_x, \vec{P}_y, \vec{P}_z\right\}$, is also centered at the center of the Earth, but with its $\vec{P}_z$ aligned with a spacecraft's orbit normal vector, its $\vec{P}_x$ pointing in the direction of the perigee, and $\vec{P}_y = \vec{P}_z \times \vec{P}_x$. This frame is specific to the orbit of a given spacecraft. As a result, two seperate perifocal frames will be used in this paper, i.e., one for each spacecraft. These frames will be denoted $\mathcal{F}_P$ and $\mathcal{F}_{P'}$ for the perifocal frame of the follower and the leader spacecraft, respectively. The corresponding unit vectors will be labeled $\left\{\vec{P}_x, \vec{P}_y, \vec{P}_z\right\}$ and $\left\{\vec{P}'_x, \vec{P}'_y, \vec{P}'_z\right\}$ for the follower and leader spacecraft, respectively.

The last reference frame relevant to this work is the local-vertical-local-horizontal (LVLH) reference frame denoted by $\mathcal{F}_L$ and defined by its orthonormal unit vectors $\left\{\vec{L}_x, \vec{L}_y, \vec{L}_z\right\}$. This reference frame has its origin at the leader spacecraft, with its $\vec{L}_x$ unit vector aligned with the spacecraft position vector and its $\vec{L}_z$ unit vector aligned with the orbit normal. The $\vec{I}_y$ unit vector completes the right-handed triad. Note that in the case of a perfectly circular orbit, $\vec{I}_y$ is in the direction of the velocity vector. The solution to the equations of motion developed in this paper provides an analytical expression of the position of the follower spacecraft with respect to the leader in $\mathcal{F}_L$.

Relative Motion on Keplerian Eccentric Orbits

As previously mentioned, previous work by Gurfil and Kholshevnikov[15,16] form a basis for the analytical solution derived herein. In their work, Gurfil and Kholshevnikov proposed a simple method of calculating the relative position of a follower spacecraft with respect to a leader using orbital elements. This allows the equations of relative motion to remain accurate for arbitrarily large values of eccentricity. To do so, consecutive rotations and a translation are applied to obtain an analytical expression for $\boldsymbol{\rho}$, defined as the components of the relative position vector in $\mathcal{F}_L$, that is

$$\boldsymbol{\rho} = \boldsymbol{r}_L - \boldsymbol{r}'_L \tag{1}$$

where $\boldsymbol{r}_L$ and $\boldsymbol{r}'_L$ respectively denote the components of the follower and leader spacecraft position vector expressed in $\mathcal{F}_L$. The first step in calculating $\boldsymbol{\rho}$ is to transform the components of the follower position vector from $\mathcal{F}_P$ to $\mathcal{F}_I$ using $\boldsymbol{C}_{IP}(\omega, i, \Omega)$, the 3-1-3 rotation sequence given by

$$\boldsymbol{C}_{IP}(\omega, i, \Omega) = \begin{bmatrix} c_\Omega c_\omega - s_\Omega s_\omega c_i & -c_\Omega s_\omega - s_\Omega c_\omega c_i & s_\Omega s_i \\ s_\Omega c_\omega + c_\Omega s_\omega c_i & -s_\Omega s_\omega - c_\Omega c_\omega c_i & -c_\Omega s_i \\ s_\omega s_i & c_\omega s_i & c_i \end{bmatrix} \tag{2}$$

where Ω, i, and ω respectively denote the right ascension of the ascending node (RAAN), inclination, and argument of perigee of the follower spacecraft. The next step is to transform the components of the follower position vector from $\mathcal{F}_I$ to $\mathcal{F}_{P'}$ using $\boldsymbol{C}_{P'I}(\omega', i', \Omega')$ given by

$$\boldsymbol{C}_{P'I}(\omega', i', \Omega') = \begin{bmatrix} c_{\Omega'} c_{\omega'} - s_{\Omega'} s_{\omega'} c_{i'} & s_{\Omega'} c_{\omega'} + c_{\Omega'} s_{\omega'} c_{i'} & s_{\omega'} s_{i'} \\ -c_{\Omega'} s_{\omega'} - s_{\Omega'} c_{\omega'} c_{i'} & -s_{\Omega'} s_{\omega'} - c_{\Omega'} c_{\omega'} c_{i'} & c_{\omega'} s_{i'} \\ s_{\Omega'} s_{i'} & -c_{\Omega'} s_{i'} & c_{i'} \end{bmatrix} \tag{3}$$

where Ω', i', and ω' denote the leader's RAAN, inclination, and argument of perigee, respectively. Then, the components of the follower position vector are rotated from $\mathcal{F}_{P'}$ to $\mathcal{F}_L$ with $\boldsymbol{C}_{LP'}(\nu')$

$$\boldsymbol{C}_{LP'}(\nu') = \begin{bmatrix} c_{\nu'} & s_{\nu'} & 0 \\ -s_{\nu'} & c_{\nu'} & 0 \\ 0 & 0 & 1 \end{bmatrix} \tag{4}$$

where ν' denotes the true anomaly of the leader spaceraft. Finally, a translation is applied, such that

$$\boldsymbol{\rho} = \boldsymbol{C}_{LP'}(v')\boldsymbol{C}_{P'I}(\omega', i', \Omega')\boldsymbol{C}_{IP}(\omega, i, \Omega)\boldsymbol{r}_P - \boldsymbol{r}'_L \tag{5}$$

where $\boldsymbol{r}_P$ and $\boldsymbol{r}'_L$ represents the components of the follower's position vector in $\mathcal{F}_P$, and the components of the leader's position vector in $\mathcal{F}_P$, respectively given by

$$\boldsymbol{r}_P = \begin{bmatrix} r\cos\nu & r\sin\nu & 0 \end{bmatrix}^T \tag{6}$$

$$\boldsymbol{r}'_L = \begin{bmatrix} r' & 0 & 0 \end{bmatrix}^T \tag{7}$$

where v denotes the true anomaly of the follower spaceraft, and where the orbit radii, r and r', are obtained from the orbit equation

$$r = \frac{a(1-e^2)}{1 + e\cos\nu} \tag{8}$$

$$r' = \frac{a'(1-e'^2)}{1 + e'\cos\nu'} \tag{9}$$

with a and e denoting the semimajor axis and eccentricity of the follower, and a' and e' denoting the semimajor axis and eccentricity of the leader spacecraft. Note that Eq. (5) can be written component-wise and further simplified through the use of relative orbital elements. For more details, the readers are referred Refs.[15,16]

Relative Motion on J_2-Perturbed Eccentric Orbits

The previous equations use constant orbital elements to calculate the position of a follower spacecraft in $\mathcal{F}_L$. Using constant orbital elements is a good approximation for the solution, and is desirable as it greatly simplifies the computations involved. The effectivenes of these equations was validated at a variety of eccentricity values, ranging from 0 to 0.8, proving that the equations are quite effective at predicting relative motion in eccentric Keplerian orbits (not shown here, for conciseness). However, perturbing accelerations will have a significant effect on the relative motion of the spacecraft. The most dominant, and therefore the most important to consider, perturbation in low-Earth orbits is the J_2 gravitational perturbation. One notable consequence of J_2 on the relative motion is a drift between both spacecraft along the $\vec{L}_y$ direction. Figure 1 shows an example of this motion for a typical satellite formation.

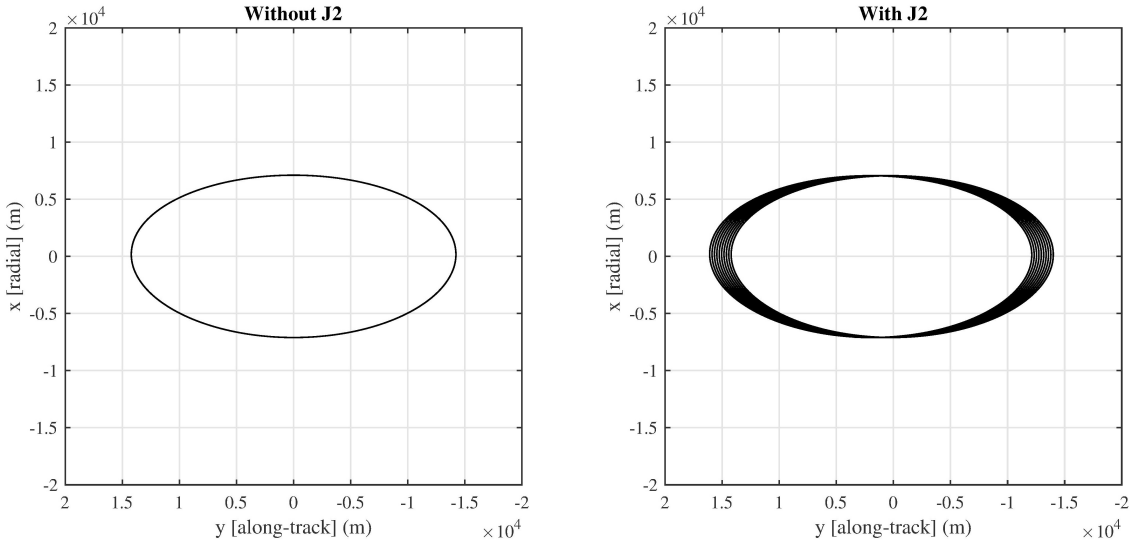

Figure 1. Simulated Relative Motion of Two Spacecraft with and without J_2 Perturbation

It should be noted, however, that Eq. (5) represents an exact solution for the relative position of the follower spacecraft at any given time, assuming that the orbital elements for each spacecraft used in the equation are accurate. Therefore, if accurate J_2-perturbed osculating orbital elements are used instead of constant ones, Eq. (5) would then result in an accurate solution for the relative position between both spacecraft under J_2. In other words, J_2-perturbed osculating orbital elements for each spacecraft can be used with Eq. (5) to accurately predict $\boldsymbol{\rho}$.

The osculating orbital elements, $[a, e, i, \omega, \Omega, M]^T$, can be accurately predicted by summing mean orbital elements with the J_2-induced short-periodic variations, as follows

$$
\begin{aligned}
a &= \bar{a} + \Delta a_{sp} \\
e &= \bar{e} + \Delta e_{sp} \\
i &= \bar{i} + \Delta i_{sp} \\
\omega &= \bar{\omega} + \Delta \omega_{sp} \\
\Omega &= \bar{\Omega} + \Delta \Omega_{sp} \\
M &= \bar{M} + \Delta M_{sp}
\end{aligned}
\tag{10}
$$

where $[\Delta a_{sp}, \Delta e_{sp}, \Delta i_{sp}, \Delta \omega_{sp}, \Delta \Omega_{sp}, \Delta M_{sp}]^T$, denote the short-periodic variations of the orbital elements, and where the mean orbital elements, $\left[\bar{a}, \bar{e}, \bar{i}, \bar{\omega}, \bar{\Omega}, \bar{M}\right]^T$, can be described as the initial mean orbital elements, denoted by $\left[\bar{a}_0, \bar{e}_0, \bar{i}_0, \bar{\omega}_0, \bar{\Omega}_0, \bar{M}_0\right]^T$, summed with the secular variations due to J_2

$$
\begin{aligned}
\bar{a} &= \bar{a}_0 \\
\bar{e} &= \bar{e}_0 \\
\bar{i} &= \bar{i}_0 \\
\bar{\omega} &= \bar{\omega}_0 + \dot{\bar{\omega}} t \\
\bar{\Omega} &= \bar{\Omega}_0 + \dot{\bar{\Omega}} t \\
\bar{M} &= \bar{M}_0 + \dot{\bar{M}} t
\end{aligned}
\tag{11}
$$

where t is the elasped time since t_0. It has been shown that the orbital elements a, e, and i have zero secular change, while the remaining elements do have some nonzero secular rate of change, denoted by $\left[\dot{\bar{\omega}}, \dot{\bar{\Omega}}, \dot{\bar{M}}\right]^T$, as a result of the J_2 perturbation[21]

$$
\dot{\bar{\omega}} = \frac{1}{2} \bar{n} J_2 \Big(\frac{R_e}{\bar{p}} \Big)^2 (4 - 5 \sin^2 \bar{i}) \tag{12}
$$

$$
\dot{\bar{\Omega}} = -\frac{3}{2} \bar{n} J_2 \Big(\frac{R_e}{\bar{p}} \Big)^2 \cos \bar{i} \tag{13}
$$

$$
\dot{\bar{M}} = \bar{n} + \frac{3}{2} \bar{n} J_2 \Big(\frac{R_e}{\bar{a}} \Big)^2 \frac{1}{(1 - \bar{e}^2)^{3/2}} \Big(1 - \frac{3}{2} \sin^2 \bar{i} \Big) \tag{14}
$$

where R_e is the mean equatorial radius of the Earth, and where the mean orbital motion and semi-latus rectum calculated with the mean semimajor axis and eccentricity, denoted as $\bar{n}$ and $\bar{p}$, respectively, are given by

$$
\bar{n} = \sqrt{\frac{\mu}{\bar{a}^3}} \tag{15}
$$

$$
\bar{p} = \bar{a}(1 - \bar{e}^2) \tag{16}
$$

Now that the mean orbital elements are fully defined for each spacecraft, the short periodic variations of each element must be calculated, as follows[20]

$$\Delta a_{sp} = \frac{J_2 R_e^2}{a}\Big[\Big(\frac{a}{r}\Big)^3 - \frac{1}{(1-e^2)^{3/2}} + \Big\{-\Big(\frac{a}{r}\Big)^3 + \frac{1}{(1-e^2)^{3/2}} + \Big(\frac{a}{r}\Big)^3\cos(2\omega+2\nu)\Big\}\frac{3\sin^2 i}{2}\Big] \tag{17}$$

$$\begin{aligned}\Delta e_{sp} =& \frac{J_2 R_e^2}{4}\Big[\frac{-2}{a^2 e\sqrt{1-e^2}} + \frac{2a(1-e^2)}{er^3} + \Big\{\frac{3}{a^2 e\sqrt{1-e^2}} - \frac{3a(1-e^2)}{er^3} - \frac{3(1-e^2)\cos(\nu+2\omega)}{p^2} \\ & - \frac{3\cos(2\nu+2\omega)}{a^2 e(1-e^2)} + \frac{3a(1-e^2)\cos(2\nu+2\omega)}{er^3} - \frac{(1-e^2)\cos(3\nu+2\omega)}{p^2}\Big\}\sin^2 i\Big]\end{aligned} \tag{18}$$

$$\Delta i_{sp} = \frac{J_2 R_e^2 \sin(2i)}{8p^2}[3\cos(2\omega+2\nu) + 3e\cos(2\omega+\nu) + e\cos(2\omega+3\nu)] \tag{19}$$

$$\Delta\Omega_{sp} = \frac{J_2 R_e^2 \cos(i)}{4p^2}[6(\nu - M + e\sin\nu) - 3\sin(2\omega+2\nu) - 3e\sin(2\omega+\nu) - e\sin(2\omega+3\nu)] \tag{20}$$

$$\begin{aligned}\Delta\omega_{sp} =& \frac{3J_2 R_e^2}{2p^2}\Big[\Big(2 - \frac{5}{2}\sin^2 i\Big)(\nu - M + e\sin\nu) \\ & + \Big(1 - \frac{3}{2}\sin^2 i\Big)\Big\{\frac{1}{e}\Big(1 - \frac{1}{4}e^2\Big)\sin\nu + \frac{1}{2}\sin(2\nu) + \frac{e}{12}\sin(3\nu)\Big\} \\ & - \frac{1}{e}\Big\{\frac{1}{4}\sin^2 i + \Big(\frac{1}{2} - \frac{15}{16}\sin^2 i\Big)e^2\Big\}\sin(\nu+2\omega) + \frac{e}{16}\sin^2 i\sin(\nu-2\omega) \\ & - \frac{1}{2}\Big(1 - \frac{5}{2}\sin^2 i\Big)\sin(2\nu+2\omega) + \frac{1}{e}\Big\{\frac{7}{12}\sin^2 i - \frac{1}{6}\Big(1 - \frac{19}{8}\sin^2 i\Big)e^2\Big\}\sin(3\nu+2\omega) \\ & + \frac{3}{8}\sin^2 i\sin(4\nu+2\omega) + \frac{e}{16}\sin^2 i\sin(5\nu+2\omega)\Big]\end{aligned} \tag{21}$$

$$\begin{aligned}\Delta M_{sp} =& \frac{3J_2 R_e^2\sqrt{1-e^2}}{2ep^2}\Big[-\Big(1 - \frac{3}{2}\sin^2(i)\Big)\Big\{\Big(1 - \frac{e^2}{4}\Big)\sin\nu + \frac{e}{2}\sin(2\nu) + \frac{e^2}{12}\sin(3\nu)\Big\} \\ & + \sin^2 i\Big\{\frac{1}{4}\Big(1 + \frac{5}{4}e^2\Big)\sin(\nu+2\omega) - \frac{e^2}{16}\sin(\nu-2\omega) - \frac{7}{12}\Big(1 - \frac{e^2}{28}\Big)\sin(3\nu+2\omega) \\ & - \frac{3e}{8}\sin(4\nu+2\omega) - \frac{e^2}{16}\sin(5\nu+2\omega)\Big\}\Big]\end{aligned} \tag{22}$$

Even though ν is not explicitly part of the orbital elements, its accurate evaluation is nevertheless required to make use of the previously defined equations. This calculation must obviously account for the J_2 perturbation, as the perturbation will have an effect on the true anomaly. In their paper, Gurfil and Kholshevnikov proposed to numerically integrate an expression for the time derivative of the true anomaly. However, doing so is undesirable. Fortunately, ν can be obtained iteratively from the mean anomaly and the orbit eccentricity through the well-known relations

$$E = M + e\sin(M + e\sin(M + e\sin(M + \cdots + e\sin(M)))) \tag{23}$$

$$\cos\nu = \frac{\cos E - e}{1 - e\cos E} \tag{24}$$

$$\sin\nu = \frac{\sqrt{1-e^2}\sin E}{1 - e\cos E} \tag{25}$$

$$\nu = \tan^{-1}\frac{\sin\nu}{\cos\nu} \tag{26}$$

where E denotes the eccentric anomaly. The number of terms in Eq. (23) is selected in accordance with the desired accuracy and is strictly a function of the magnitude of the eccentricity.

PROCEDURE FOR FINDING RELATIVE MOTION SOLUTION

In the previous section, all of the necessary equations were presented for solving analytically for the relative position between two spacecraft, i.e., by using Eq. (5) with J_2-perturbed osculating orbital elements. The purpose of this section is to summarize the steps taken to apply these equations to propagate the relative position vector.

1. Two sets of Keplerian initial osculating orbital elements are specified, i.e., $[a_0, e_0, i_0, \omega_0, \Omega_0, \nu_0]^T$ and $[a_0', e_0', i_0', \omega_0', \Omega_0', \nu_0']^T$.

2. The mean anomaly of each spacecraft most also be initialized, i.e., M_0 and M_0'. This is accomplished by working backwards from the true anomaly to the eccentric anomaly and finally mean anomaly using Eqs. (23)-(26).

3. The initial short-periodic variations for each spacecraft are calculated as a function of the initial osculating orbital elements using Eqs. (17)-(22).

4. By rearranging Eq. (10), the initial mean orbital elements for each spacecraft can then be calculated from the initial short-periodic variations subtracted from the initial osculating orbital elements, that is

$$\begin{aligned}
\bar{a}_0 &= a_0 - \Delta a_{0_{sp}} \\
\bar{e}_0 &= e_0 - \Delta e_{0_{sp}} \\
\bar{i}_0 &= i_0 - \Delta i_{0_{sp}} \\
\bar{\omega}_0 &= \omega_0 - \Delta\omega_{0_{sp}} \\
\bar{\Omega}_0 &= \Omega_0 - \Delta\Omega_{0_{sp}} \\
\bar{M}_0 &= M_0 - \Delta M_{0_{sp}}
\end{aligned}$$

and similarly for the leader spacecraft.

5. The mean semimajor axis, eccentricity and inclination have no secular variation, and are therefore equal to their initial mean values, as calculated in the previous step, i.e., $\bar{a} = \bar{a}_0$, $\bar{e} = \bar{e}_0$, and $\bar{i} = \bar{i}_0$, as well as $\bar{a}' = \bar{a}'_0$, $\bar{e}' = \bar{e}'_0$, and $\bar{i}' = \bar{i}'_0$. The mean orbital motion and mean semilatus rectum for each spacecraft, $\bar{n}$, $\bar{p}$, $\bar{n}'$, and $\bar{p}'$, may also be calculated at this point using Eqs. (15) and (16), as these parameters are only functions of mean semimajor axis and mean eccentricity.

6. The remaining mean orbital elements, $\left[\bar{\omega}, \bar{\Omega}, \bar{M}\right]^T$ and $\left[\bar{\omega}', \bar{\Omega}', \bar{M}'\right]^T$, can be propagated forward in time, from t_0 to t, using Eqs. (12)-(14) with Eq. (11).

7. Based on the average mean anomalies, $\bar{M}$ and $\bar{M}'$, the true anomaly for each spacecraft, ν and ν', are propagated forward in time using Eqs. (23)-(26).

8. Now that the true anomalies have been propagated forward in time, the short-periodic variations can then be calculated for each spacecraft using Eqs. (17)-(22). The osculating orbital elements are then propagated forward in time using Eq. (10).

9. Finally, $\boldsymbol{\rho}$ is obtained through Eq. (5), with rotation matrices in Eqs. (2)-(4) and position vectors in Eqs. (6) and (7) evaluated with the J_2-perturbed osculating orbital elements.

NUMERICAL SIMULATIONS

To verify the accuracy of the newly developed method of calculating the relative position between two spacecraft, numerical simulations were performed in MATLAB. The results obtained with the analytical solution provided in this paper were compared to a numerical simulator that integrates the exact, nonlinear differential equations of motion in $\mathcal{F}_I$. Specifically, the simulator integrates, for each spacecraft, the inertial two-body equations of motion to which the J_2 inertial perturbing acceleration was added. Both spacecraft's position vectors are then transformed into $\mathcal{F}_L$. Finally, the leader position vector is subtracted from the follower position vector, to obtain $\boldsymbol{\rho}$, the components of the exact relative position vector in $\mathcal{F}_L$. The simulator was initialized using, for both spacecraft, the initial osculating orbital elements which were converted into components of the initial position and velocity vectors in $\mathcal{F}_I$. The exact same initial osculating orbital elements were also used to initialize the proposed method of calculating relative position outlined in the previous section. Unless otherwise specified in the captions of the subsequent figures, Table 1 presents the initial osculating orbital elements used for both models (numerical simulator and analytical equations). The orbital elements given in this Table correspond to a simple in-plane elliptical formation.

Table 1. Initial Osculating Orbital Elements

Orbital Element	Leader	Follower
Semimajor Axis (km)	7106.14	7106.14
Eccentricity	0.05	e' + 0.001
Inclination (deg)	98.3	98.3
Argument of Perigee (deg)	0	0
Right Ascension of Ascending Node (deg)	270	270
True Anomaly (deg)	0	0

Figure 2 reports the results obtained by propagating the relative motion at a relatively low eccentricity over six orbits with the analytical equations and the numerical simulator. As shown, the position error, defined as difference between the analytical solution and the numerical simulator,

remains bounded (for all practical purposes) with an accuracy better than 5 meters along each direction. While there is a slight increase in the error in the along-track direction, this minimal drift is negligible over the six orbital periods shown.

Figures 3 and 4 show the results obtained when the leader reference orbit is significantly more elliptical. Similarly to the previous near-circular orbit case, the errors are bounded, and the analytical solution is representative of the exact spacecraft motion. However, it is clear that as the eccentricity increases the ability of the analytical solution to track the relative motion accurately decreases. This is especially true in the along-track direction, where the error increases significantly with increase in eccentricity.

Proving that the new analytical solution can predict relative postion in highly eccentric orbits is particularly important. To this end, a simulation was performed with $e' = 0.8$. Figure 5 shows that the analytical equations do begin to show unbounded error at such high eccentricity values, with large error spikes reaching several kilometers after six orbits. Looking at the left side of Figure 5 it can be seen that the analytical solution still models the simulated motion well despite the increasing error, and it can also be seen that over time, as the satellites drift apart due to J_2, the errors get worse. It should be noted that accuracy of Eq. (23) is a function of the number of iterations performed in the equation. When the eccentricity was increased to 0.8, the resulting errors were initially significantly larger. By increasing the iterations in Eq. (23) this error was reduced to the results shown in Figure 5. To further study the application of the proposed analytical solution for formations on highly-eccentric orbits, the relative equations of motion were applied to the upcoming European Space Agency PROBA-3 mission. This Sun observation mission will involve two spacecraft in precise formation in highly-eccentric orbits, with the formation forming a solar coronagraph. The PROBA-3 leader's orbit is defined with a'_0 = 37040 km, e'_0 = 0.806, i'_0 = 59 deg, Ω'_0 = 84 deg, and ω'_0 = 188 deg, as well as a spacecraft speration on the order of 100 meters.[22] Setting up a simulation with two spacecraft in this orbit, with the follower eccentricity given by $e = e' + 0.00005$ is a gross simplification of the ultimate relative motion for the mission, but it may still provide some insight regarding the accuracy of the proposed analytical solution in a realistic mission scenario. Figure 6 shows the results of the simulation. Although the resulting errors are unbounded, the error is controlled quite well, staying below 40 meters over six orbital periods.

In each of the previous cases, the formation was defined such that there is no out-of-plane motion. As it is important to assess the ability of the analytical solution to handle out-of-plane motion effectively, three more cases were simulated at varying inclination differences between the two spacecraft. The results, in order of increasing inclination difference are reported in Figures 7, 8, and 9.

CONCLUSION

A set of nonlinear analytical equations for the relative motion between two spacecraft in formation which is applicable to a wide variety of orbits, and also takes into account the J_2 perturbation was derived in this paper. By building upon previously-published results, the relative motion is formulated as a function of osculating J_2-perturbed orbital elements, such that an analytical solution that is exact for a perturbed orbit of any shape was used. This new method of obtaining the relative position between two spacecraft in formation was validated in numerical simulations. When compared to a numerical simulator, the analytical solution follows the simulated motion accurately along all three directions, and the relatively small errors are bounded for most cases. Future work will focus on reformulating the proposed analytical solution into component-wise equations. This

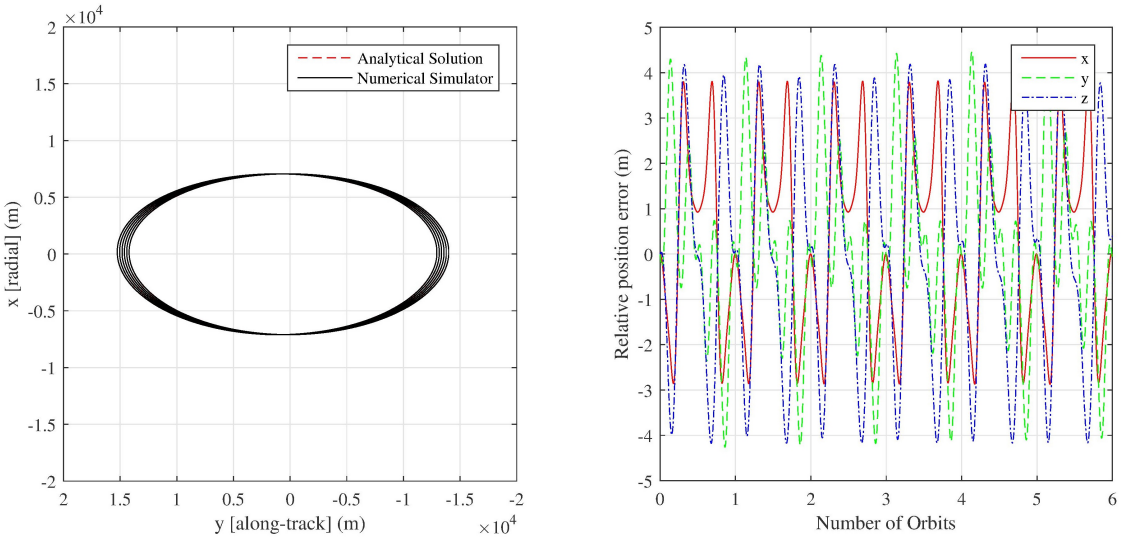

Figure 2. Analytical Solution Compared with Numerical Simulator

could potentially decrease the computational resources required to use the proposed analytical solution in an on-board guidance system. Additionally, in practice, it is likely not desired to have two spacecraft drifting apart due to the J_2 perturbation. Further examination of the analytical equations in a component-wise form would allow the elimination of this drift by careful selection of the initial osculating orbital elements. This would be analogous to establishing the formation in a widely-used J_2-invariant orbit.

ACKNOWLEDGMENTS

This work was financially supported by the Natural Sciences and Engineering Research Council of Canada under the Undergraduate Student Research Award Program and Discovery Grant Program. Special thanks to John and Lorna Kuiack for all of their support, and Giuliana Velarde for all of her editing help.

REFERENCES

[1] W. H. Clohessy and R. S. Wiltshire, "Terminal Guidance System for Satellite Rendezvous," *Journal of the Aerospace Sciences*, Vol. 27, No. 9, 1960, pp. 653–658.

[2] C. Sabol and C. A. McLaughlin, "Satellite Formation Flying Design and Evolution," *Journal of Spacecraft and Rockets*, Vol. 38, No. 2, 2001, pp. 270–278.

[3] S. A. Schweighart and R. J. Sedwick, "High-Fidelity Linearized J_2 Model for Satellite Formation Flight," *Journal of Guidance, Control, and Dynamics*, Vol. 25, No. 6, 2002, pp. 1073–1080.

[4] G. Inalhan, M. Tillerson, , and J. How, "Relative Dynamics and Control of Spacecraft Formations in Eccentric Orbits," *Journal of Guidance, Control, and Dynamics*, Vol. 25, No. 1, 2002, pp. 48–59.

[5] H. Schaub, "Relative Orbit Geometry Through Classical Orbit Element Differences," *Journal of Guidance, Control, and Dynamics*, Vol. 27, No. 5, 2004, pp. 839–848.

[6] R. A. Broucke, "Solution of the Elliptic Rendezvous Problem with the Time as Independant Variable," *Journal of Guidance, Control, and Dynamics*, Vol. 26, No. 4, 2003, pp. 615–621.

[7] D. J. Zanon and M. E. Campbell, "Optimal Planner for Spacecraft Formations in Elliptical Orbits," *Journal of Guidance, Control, and Dynamics*, Vol. 29, No. 1, 2006, pp. 161–171.

[8] L. Breger, G. Inalhan, M. Tillerson, and J. How, "Cooperative Spacecraft Formation Flying: Model Predictive Control with Open- and Closed-Loop Robustness," *Modern Astrodynamics* (P. Gurfil, ed.), ch. 8, pp. 237–277, Elsevier Astrodynamics Series, 2006.

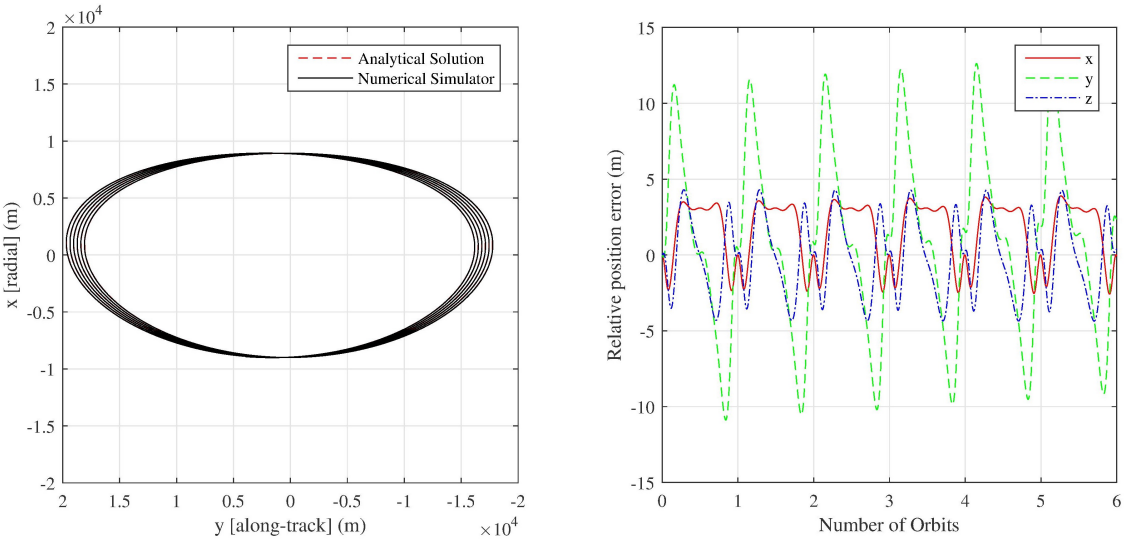

Figure 3. Analytical Solution Compared with Numerical Simulator for $e' = 0.2$ and $a' = 9,000$ km

[9] T. E. Carter and M. Humi, "Fuel-Optimal Rendezvous near a Point in General Keplerian Orbit," *Journal of Guidance, Control, and Dynamics*, Vol. 10, No. 6, 1987, pp. 567–573.

[10] D. Lawden, *Optimal Trajectories for Space Navigation*. Butterworths, 1963.

[11] T. E. Carter, "New Form for the Optimal Rendezvous Equations near a Keplerian Orbit," *Journal of Guidance, Control, and Dynamics*, Vol. 13, No. 1, 1990, pp. 183–186.

[12] J. P. Marec, *Optimal Space Trajectories*. Elsevier, 1979.

[13] C. Lane and P. Axelrad, "Formation Design in Eccentric Orbits Using Linearized Equations of Relative Motion," *Journal of Guidance, Control, and Dynamics*, Vol. 29, No. 1, 2006, pp. 146–160.

[14] R. G. Melton, "Time-Explicit Representation of Relative Motion Between Elliptical Orbits," *Journal of Guidance, Control, and Dynamics*, Vol. 23, No. 4, 2000, pp. 604–610.

[15] P. Gurfil and K. V. Kholshevnikov, "Distances on the Relative Spacecraft Motion Manifold," *AIAA Guidance, Navigation and Control Conference and Exhibit*, San Francisco, CA, 2005. AIAA paper 2005-5859.

[16] P. Gurfil and K. V. Kholshevnikov, "Manifolds and Metrics in the Relative Spacecraft Motion Problem," *Journal of Guidance, Control, and Dynamics*, Vol. 29, No. 4, 2006, pp. 1004–1010.

[17] G. W. Hill, "Researches in the Lunar Theory," *American Journal of Mathematics*, Vol. 1, 1878, pp. 5–26.

[18] P. Gurfil and N. J. Kasdin, "Nonlinear Modeling of Spacecraft Relative Motion in the Configuration Space," *Journal of Guidance, Control, and Dynamics*, Vol. 27, No. 1, 2004, pp. 154–157.

[19] H. Schaub, "Incorporating Secular Drifts into the Orbit Element Difference Description of Relative Orbits," *Advances in the Astronautical Sciences*, Vol. 114, 2003, pp. 239–258.

[20] D. Brouwer, "Solution of the Problem of Artificial Satellite Theory without Drag," *The Astronomical Journal*, Vol. 64, No. 1274, 1959, pp. 378–396.

[21] D. A. Vallado, *Fundamentals of Astrodynamics and Applications*, pp. 604–612. El Segundo, CA: Microcosm Press, 2 ed., 2001.

[22] J. S. Llorente, A. Agenjo, C. C., C. d. Negueruela, A. Mestreau-Garreau, A. Cropp, and A. Santovincenzo, "PROBA-3: Precise Formation Flying Demonstration Mission," *Acta Astronautica*, Vol. 82, No. 1, 2013, pp. 388–46.

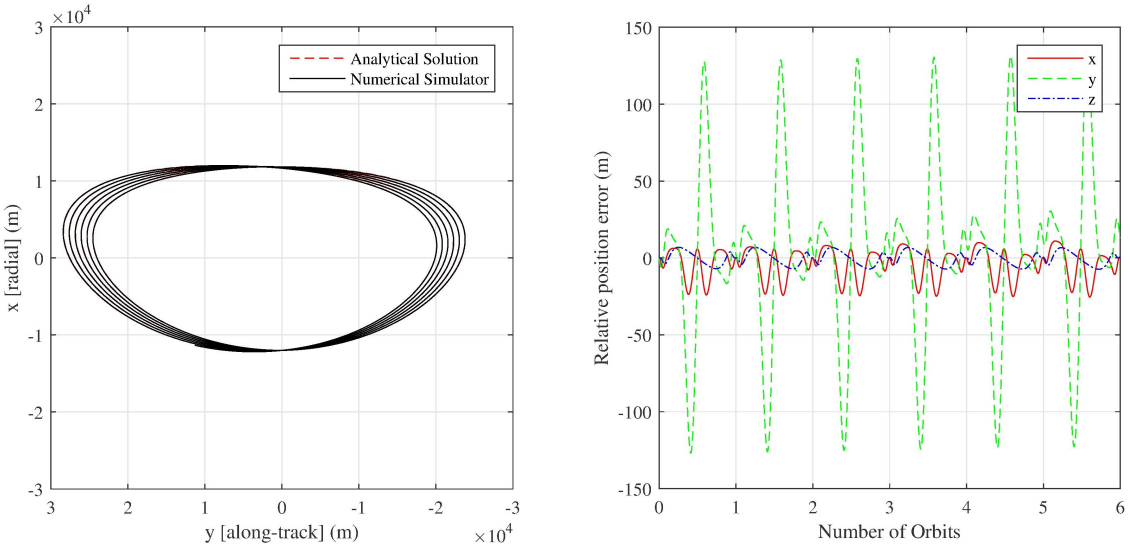

Figure 4. Analytical Solution Compared with Numerical Simulator for $e' = 0.4$ and $a' = 12,000$ km

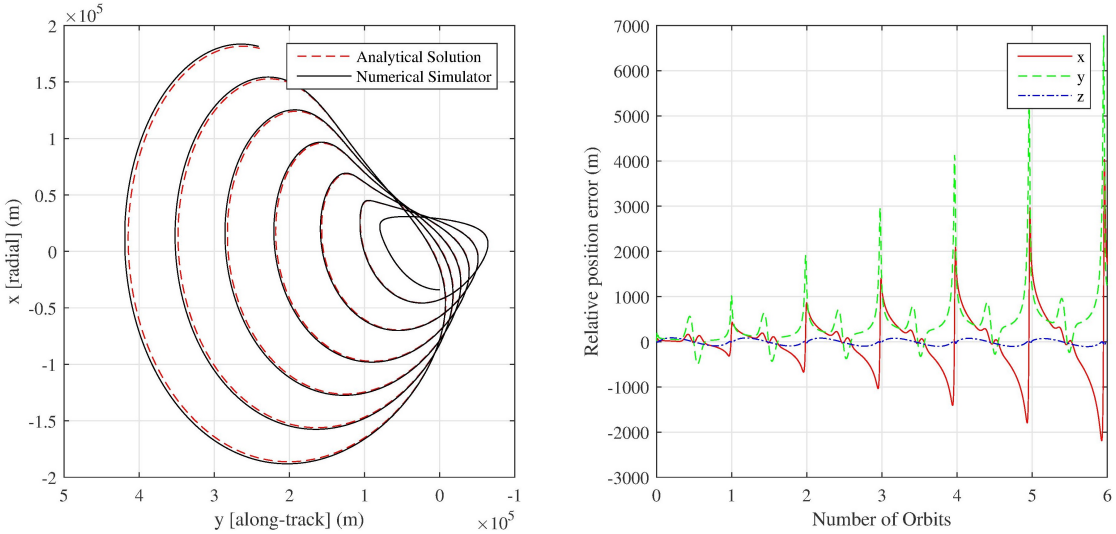

Figure 5. Analytical Solution Compared with Numerical Simulator for $e' = 0.8$ and $a' = 34,000$ km

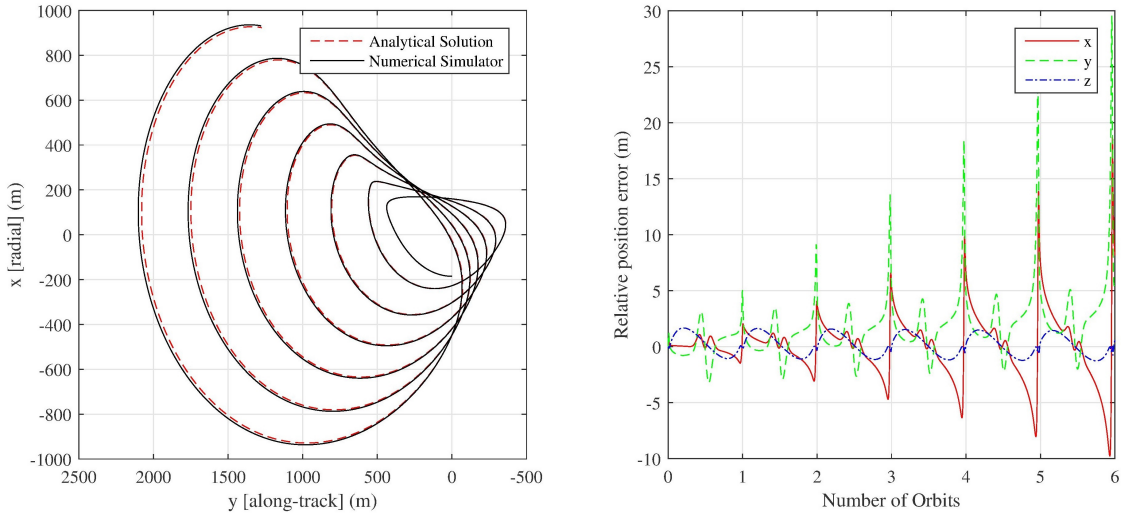

Figure 6. Analytical Solution Compared with Numerical Simulator for PROBA-3 example

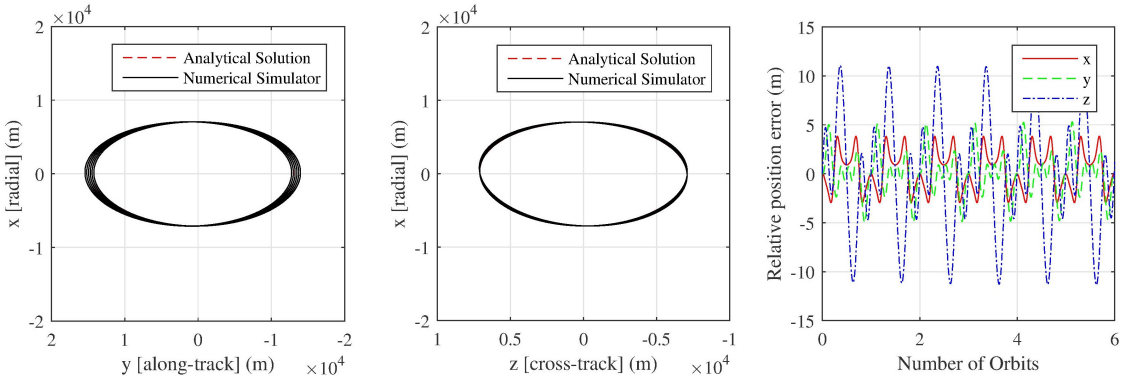

Figure 7. Analytical Solution Compared with Numerical Simulator for $i = i' + 0.001$ deg

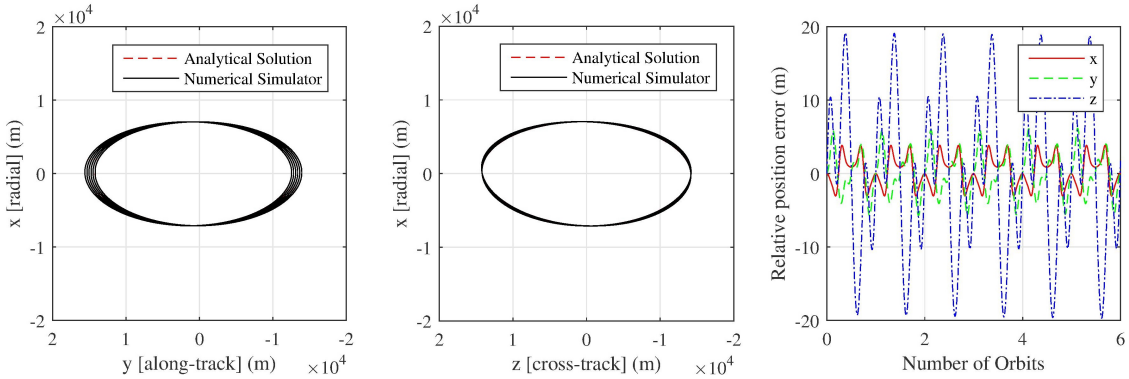

Figure 8. Analytical Solution Compared with Numerical Simulator for $i = i' + 0.002$ deg

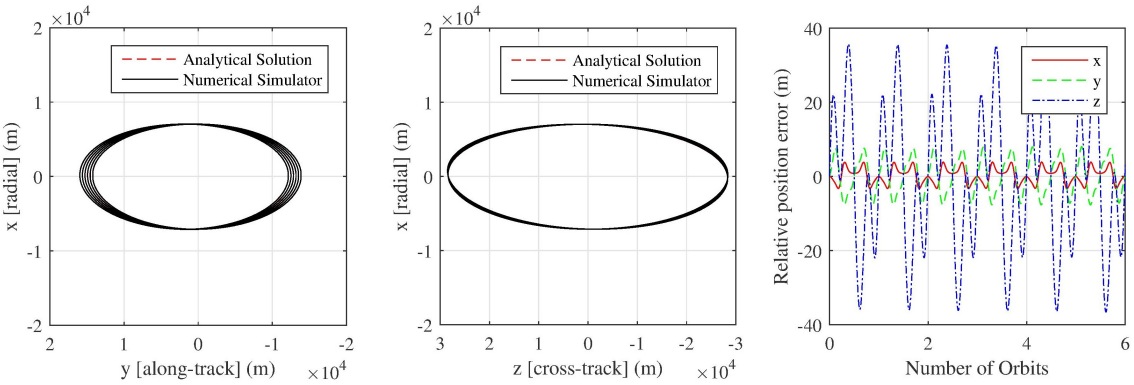

Figure 9. Analytical Solution Compared with Numerical Simulator for $i = i' + 0.004$ deg